Journal of Solid State Chemistry 184 (2011) 2405–2411

Contents lists available at ScienceDirect

Journal of Solid State Chemistry

journal homepage: www.elsevier.com/locate/jssc

Self-assembly of Fe_3O_4 nanocrystal-clusters into cauliflower-like architectures: Synthesis and characterization

Lu-Ping Zhu [a,*], Gui-Hong Liao [b], Nai-Ci Bing [a], Lin-Lin Wang [a], Hong-Yong Xie [a]

[a] School of Urban Development and Environmental Engineering, Shanghai Second Polytechnic University, Shanghai 201209, China
[b] Technical Institute of Physics and Chemistry, Chinese Academy of Sciences, Beijing 100190, China

ARTICLE INFO

Article history:
Received 18 January 2011
Received in revised form
8 July 2011
Accepted 11 July 2011
Available online 20 July 2011

Keywords:
Self-assembly
Architectures
Magnetite
Magnetic properties

ABSTRACT

Large-scale cauliflower-like Fe_3O_4 architectures consist of well-assembled magnetite nanocrystal clusters have been synthesized by a simple solvothermal process. The as-synthesized Fe_3O_4 samples were characterized by XRD, XPS, FT-IR, SEM, TEM, etc. The results show that the samples exhibit cauliflower-like hierarchical microstructures. The influences of synthesis parameters on the morphology of the samples were experimentally investigated. Magnetic properties of the Fe_3O_4 cauliflower-like hierarchical microstructures have been detected by VSM at room temperature, showing a relatively low saturation magnetization of 65 emu/g and an enhanced coercive force of 247 Oe.

1. Introduction

During the past few years, the synthesis and characterization of nanoscale magnetic materials have aroused extensive attention as the materials in this size would allow investigating the fundamental aspects of magnetic-ordering phenomena in magnetic materials with reduced dimensions and could also lead to new potential applications such as high-density recording media, magnetic sensors, and so forth [1]. Magnetite (Fe_3O_4) is one of the most important magnetic materials and has been widely used in electronic devices, information storage, magnetic resonance imaging (MRI), and drug-delivery technology [2–6]. To date, various nanostructures of magnetites, such as nanorods [7,8], nanowires [9,10], nanotubes [11], nanopyramids [12], nanooctahedra [13–15], hollow microspheres [16,17], and flower-like nanostructures [18–21] have been prepared by a variety of methods, including reverse-micelle transition, hydro/solvothermal treatment, magnetic-field induction, wet-chemical etching, chemical vapor deposition, and polyol-mediated process. Although Fe_3O_4 nanocrystallites with different morphologies [7–23] were synthesized previously, to the best of our knowledge, there are few reports on the synthesis of complex structure Fe_3O_4 architectures without any surfactants or templates through a solution-based approach. The exploration of mild synthetic methods of magnetic materials with controllable size and morphology at moderate temperature without surfactants or templates remains an important challenge.

In this study, we present a facile solution-phase approach to cauliflower-like Fe_3O_4 hierarchical microstructures in ethylene glycol (EG) solution without employing any surfactants or templates. The advantages of this method are that long time is not required for crystal growth, cheap inorganic salts are used as raw materials, and reaction conditions is easily controlled for mass production. The phase purity, shape, size, and structure of the as-prepared samples are characterized using XRD, SEM, TEM, etc. Magnetic measurements at room temperature indicate that the saturation magnetization and the coercivity of cauliflower-like Fe_3O_4 hierarchical microstructures are 65 emu/g and 247 Oe, respectively. These Fe_3O_4 architectures may have potential applications in catalysis, magnetic, biological, and sensing related fields.

2. Experimental

Iron(III) chloride hexahydrate ($FeCl_3 \cdot 6H_2O$), ethylenediamine (EDA), ethylene glycol (EG), and ethanol were purchased from Beijing Chemical Reagent Ltd. (Beijing, China) and used as received without further purification. In a typical experiment, 30 mL solution consisting of $FeCl_3 \cdot 6H_2O$ was prepared by dissolving $FeCl_3 \cdot 6H_2O$(1.35 g) in EG. Subsequently, 6 mL ethylenediamine (EDA) was added drop-wise into the above solution and the mixture was stirred for an additional 1 h at room temperature. Then, the mixture was transferred into a Teflon-lined stainless-steel autoclave of 50 mL capacity. The autoclave was sealed and

* Corresponding author. Fax: +86 21 50216301.
E-mail addresses: lpzhu@eed.sspu.cn, lpzhu@mail.ipc.ac.cn (L.-P. Zhu).

0022-4596/$ - see front matter © 2011 Elsevier Inc. All rights reserved.
doi:10.1016/j.jssc.2011.07.013

maintained at 200 °C for 12 h and then was cooled to room temperature. A sample in powder form was obtained by centrifuging, sequentially rinsing with ethanol for several times, and then dried in a vacuum oven at 60 °C for 6 h.

The phase purity of the product was examined by X-ray diffraction (XRD) using a Rigaku *D*/max 2500 diffractometer with Cu-*K*α radiation (λ=1.5406 Å). X-ray photoelectron spectroscopy (XPS) data were obtained with an ESCALab220i-XL electron spectrometer from VG Scientific using 300 W Al *K*α radiation. The binding energies were referenced to the C1*s* line at 284.8 eV from adventitious carbon. Scanning electron microscopy (SEM) images and X-ray energy dispersive spectroscopy (EDS) analyses were performed using a Hitachi S-4800 microscope (Japan). Transmission electron microscopy (TEM) images and the corresponding selected area electron diffraction (SAED) pattern were taken on a FEI Tecnai G2 20 transmission electron microscope. Fourier transform infrared (FT-IR) spectrum was recorded with a Varian 3100 FT-IR spectrometer using a KBr wafer. Magnetic measurement for the samples in the powder form was carried out at room temperature using a vibrating sample magnetometer (VSM, Lakeshore 7307, USA) with a maximum magnetic field of 10 kOe.

3. Results and discussion

Fig. 1a is the typical XRD pattern of the sample obtained at 200 °C for 12 h in ethylene glycol (EG) solution, using $FeCl_3 \cdot 6H_2O$ and EDA as the starting materials. It is clearly noticed that all diffraction peaks in the XRD pattern can be perfectly indexed as face-centered cubic Fe_3O_4 with lattice constant a=0.8390 nm, which is very close to the reported data (JCPDS 85-1436). No other peaks of impurities could be found in the XRD pattern. The peaks shown in the XRD pattern are sharp and intense, indicating good crystallinity. Fig. 1b shows representative XPS spectrum of the prepared product. The photoelectron peaks at 711.7 and 725.2 eV are the characteristic doublet of Fe $2p_{3/2}$ and $2p_{1/2}$ core-level spectra of iron oxide, respectively, which is consistent with the oxidation state of Fe in Fe_3O_4. Fig. 1c exhibits FT-IR spectrum of as-synthesized cauliflower-like Fe_3O_4 hierarchical microstructures. The strong absorption band around 575 cm^{-1} is assigned to Fe–O stretching vibration modes, proving the existence of Fe_3O_4 [24,25]. The band at 1627.4 cm^{-1} ($-NH_2$) found in Fig. 1c indicates the existence of the free $-NH_2$ group on the magnetites.

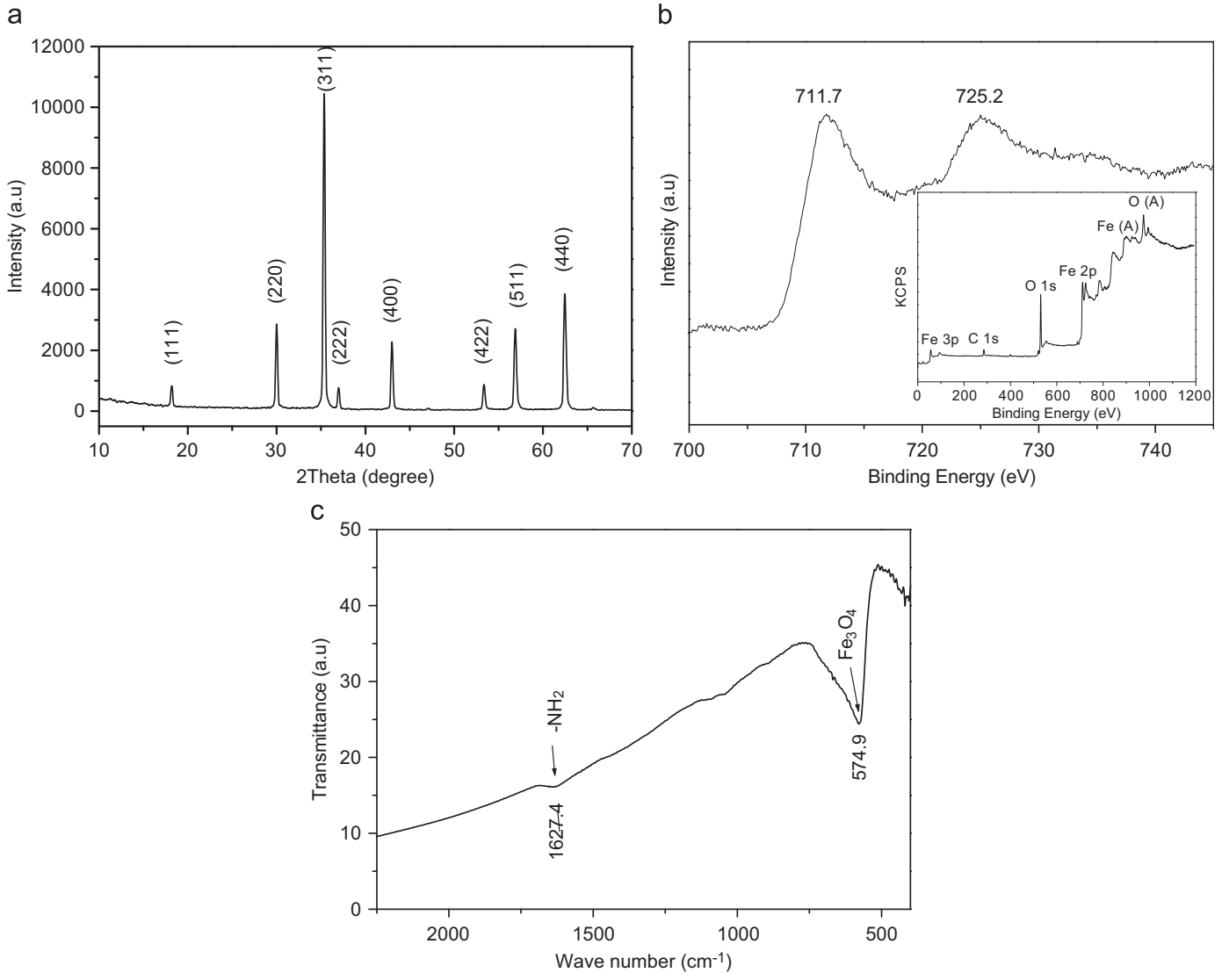

Fig. 1. (a) XRD pattern and (b) X-ray photoelectron spectra of the as-prepared samples in the presence of EDA at 200 °C for 12 h, (c) FT-IR spectrum of the magnetites obtained in the presence of EDA.

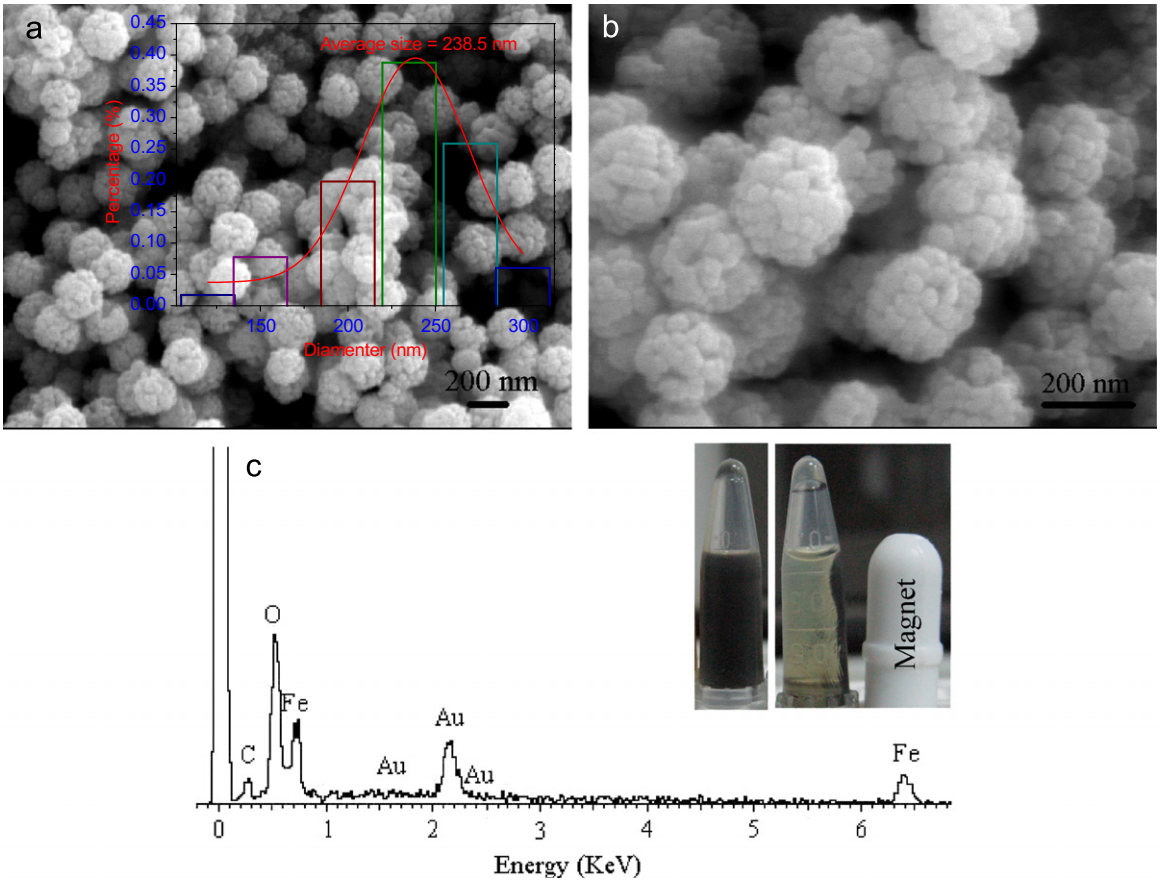

Fig. 2. (a) Low-magnification SEM image of the large-scale self-assembled cauliflower-like Fe_3O_4 hierarchical microstructures dispersing harmoniously. Inset of (a): the size distribution of the as-synthesized samples, (b) high-magnification SEM image of the cauliflower-like Fe_3O_4 hierarchical microstructures, (c) EDS result of the cauliflower-like Fe_3O_4 hierarchical microstructures. The inset photographs in (c) show that the as-synthesized Fe_3O_4 sample can be easily dispersed in water and also be drawn from the solution to the sidewall of the vial by an assistant magnet field.

The SEM images of the as-synthesized Fe_3O_4 samples obtained at 200 °C for 12 h are shown in Fig. 2. Clearly, the products consist of a high yield of uniform Fe_3O_4 particles ranging in size from 200 to 300 nm (Fig. 2a), showing a relatively narrow size distribution (inset of Fig. 2a). The magnified SEM image showed in Fig. 2b displays that the Fe_3O_4 particles have cauliflower-like hierarchical microstructures, which are built from several dozen of nanocrystal clusters with size of 20–50 nm. The as-prepared products were also determined by EDS analysis under N_2 atmosphere. The EDS result shown in Fig. 2c demonstrates that the as-prepared samples contain Fe and O with the Fe/O atomic ratio of ~3:4, which agrees well with the expected stoichiometry. The presence of C could come from the conducting resin during measurements.

Further observation on the structure of the as-synthesized Fe_3O_4 samples was conducted by TEM (Fig. 3a). In agreement with the above SEM findings, a cauliflower-like hierarchical microstructure can be seen from the image. The corresponding SAED pattern taken from an individual cauliflower-like Fe_3O_4 hierarchical microstructure is shown in Fig. 3b. It is interesting that the assembled structure with nanocrystal clusters exhibits an almost single-crystalline diffraction pattern, which can be indexed to the face-centered cubic structure with phase purity [26,27]. Fig. 3c shows the enlarged TEM image of the edge area of one individual cauliflower-like Fe_3O_4 hierarchical microstructure. The high-resolution TEM (HRTEM) images of the different areas marked by rectangles are demonstrated in Fig. 3d and e. The clear lattice image indicates the high crystallinity and single-crystalline nature of the Fe_3O_4 hierarchical microstructure. A lattice spacing of 0.49 nm for the (1 1 1) planes can be readily resolved.

The morphology of as-synthesized Fe_3O_4 samples is distinctly different from the nanotubes, nanowires, and nanorods. Template synthesis is a general approach to obtain complex structured micro/nanomaterials. However, in this work, cauliflower-like Fe_3O_4 hierarchical microstructures were synthesized in EG solution without employing any surfactants or templates, thus EDA may play an important role in the formation of cauliflower-like hierarchical structures. As we known, EDA is an important ligand for metal ions and has been widely employed as a shape controller and stabilizer in the synthesis of fine handkerchief-like Ni and NiCo nanoalloys [28], ZnSe flowerlike nanoarchitectures [29], hollow CdS nanoboxes [30], hexagonal, star-shaped and snowflake-shaped Cu structures [31], dendrite-like SnS [32], nanorods and flowerlike ZnO structures [33].

In order to investigate the effect of EDA on the formation, morphology, and structure of the as-obtained products, controlled experiments were conducted. With other synthetic conditions held constant, adjusting the amount of EDA led to an obvious shape evolution of Fe_3O_4 particles from solid microspheres to hollow microspheres, cauliflower-like hierarchical microstructures and inhomogeneous micro/nanoparticles as shown in Fig. 4. It has been proved that the concentration or amount of surfactant can dramatically affect the evolution of the shape of inorganic crystals. When the amount of EDA was 0.8 mL in the solution, the Fe_3O_4 solid spheres were obtained as dominant product (Fig. 4a). When the amount of EDA increased up to 3.0 mL, the high yield of Fe_3O_4 hollow spheres was obtained (Fig. 4b). When the EDA amount was increased to 6.0 mL, the nanoparticles serving as building blocks began to exhibit a strong

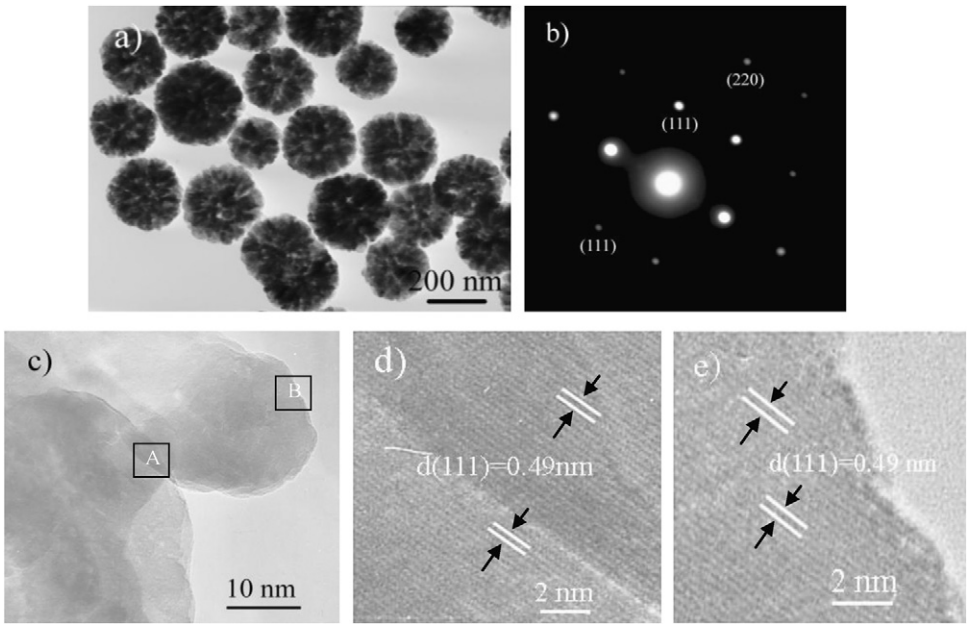

Fig. 3. (a) TEM image of cauliflower-like Fe_3O_4 hierarchical microstructures, (b) the corresponding SAED pattern taken from an individual cauliflower-like Fe_3O_4 hierarchical microstructure, (c) enlarged TEM image obtained from the edge area of one individual cauliflower-like Fe_3O_4 hierarchical microstructure, (d) HRTEM image of A area (indicated by a rectangle in c), and (e) HRTEM image of B area (indicated by a rectangle in c).

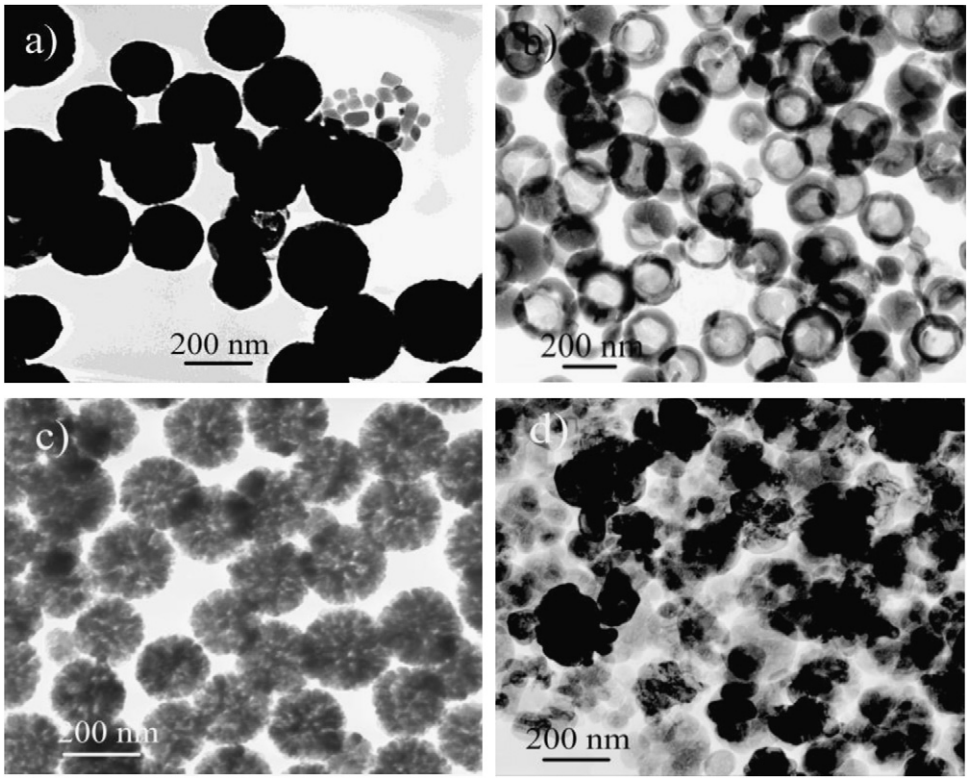

Fig. 4. TEM micrographs of the samples prepared at 200 °C for different amount of EDA: (a) 0.8 mL, (b) 3 mL, (c) 6 mL, and (d) 10 mL.

tendency to assemble into cauliflower-like hierarchical microstructures under the experimental conditions (see Fig. 4c). However, when the amount of EDA was more than 6 mL, the cauliflower-like hierarchical microstructures disappeared, and inhomogeneous micro/nanoparticles were also obtained (Fig. 4d).

Besides the amount of EDA, the shape, and structure of as-synthesized samples were also affected by other synthesis parameters such as synthesis temperature, time, etc. For example, when the temperature was lower than 200 °C, no magnetite can be obtained. To investigate the formation process of the cauliflower-like hierarchical microstructures, time-dependent experiments were carried out. The results showed that the reaction duration was also found to be an another important factor. Our time-dependent experiments revealed that only yellow rather than black precipitates could be obtained when the reaction time was less than or equal to 8 h (Fig. 5a). The TEM image shown in

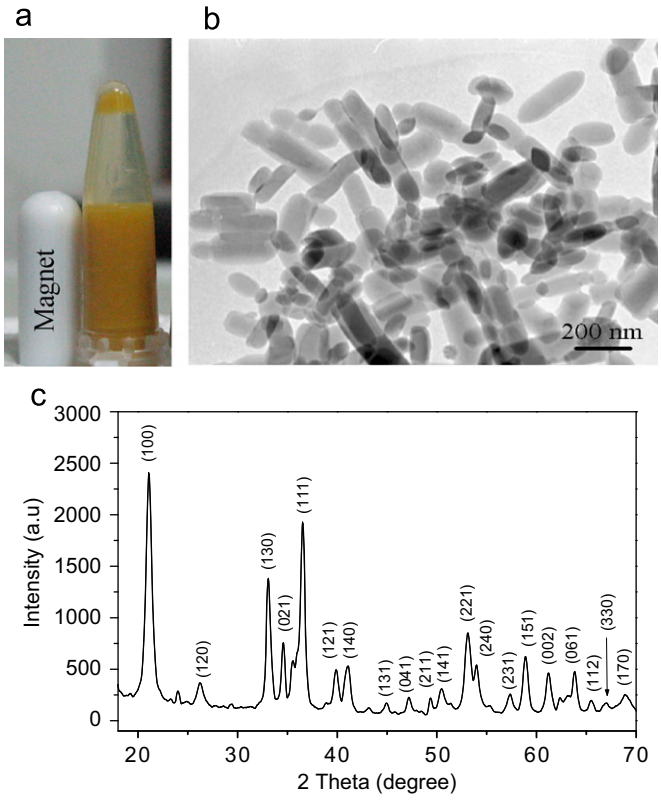

Fig. 5. (a) Suspension, (b) TEM image, and (c) XRD pattern of the as-prepared samples in the presence of EDA at 200 °C for 6 h.

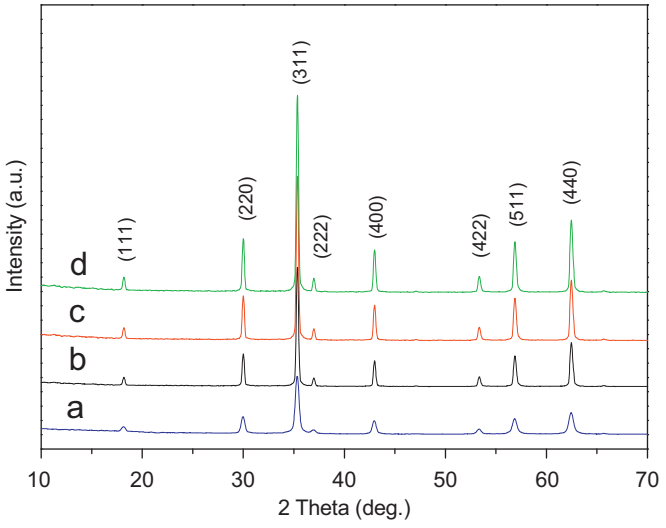

Fig. 6. XRD patterns of the products obtained at different reaction times: (a) 8.5 h, (b) 10 h, (c) 12 h, and (d) 16 h.

Fig. 5b displays that the samples obtained in the presence of EDA at 200 °C for 6 h have a rod-like structure. Based on the XRD result (see Fig. 5c), the above-obtained yellow sample shows the pure phase of α-FeOOH. When the time was increased to 8.5 h we could acquire brownish-black precipitation. The peaks belonged to spinel Fe_3O_4 appeared on the XRD pattern (Fig. 6a), implying the start of crystallization. The TEM image shown in Fig. 7a displays the product consisted of solid spheres with diameters about 150 nm. Extending the time to 10 h, the crystallinity of the product was increased (Fig. 6b), at the same time, we could observe that the spheres grew larger continuously (Fig. 7b), indicating that assembly is still underway. Careful observation of a single sphere revealed that the sphere was constructed of a large number of nanoparticles. As the reaction time went on to 12 h, the products were completely transformed into well-crystallized cauliflower-like hierarchical microstructures (Figs. 6c and 7c). Further prolonging the reaction time to 16 h, the intensity of all the peaks belonging to the spinel Fe_3O_4 increased (Fig. 6d), suggesting that the longer reaction time favors the crystallization of the Fe_3O_4 phase. Careful comparison of Fig. 7c and d revealed that the microstructures were increased to about 250 nm and the sizes of nanocrystal clusters obviously became larger (Fig. 7d). Of course, similar to the previous reports in the literature, all the parameters for the controlled synthesis of nanocrystals under solvothermal conditions should be interdependent, thus resulting in interesting combinations for the shape-selective synthesis of various Fe_3O_4 particles.

On the basis of the above results, a possible formation process can be schematically illustrated in Fig. 8. In our synthesis, Fe^{3+} in EG solution reacted first with EDA to form a relatively stable octahedral structure of Fe^{3+}–EDA complex under ambient conditions. The formation of $Fe(EDA)_3^{3+}$ sharply decreased the free Fe^{3+} concentration in the solution, resulting in a relatively slow formation rate of FeOOH. A slow formation rate led to the separation of nucleation and growth steps, which is crucial for synthesis of high-quality crystal. Afterwards, at a relatively high temperature and auto-generated vapor pressure, the complex decomposed and released EDA. As a result, the rod-like FeOOH was firstly formed. As the reaction proceeded, the FeOOH nanoparticles may re-dissolve in the solution and react with Fe^{2+} from the reduction of Fe^{3+} in EG solution at 200 °C to form Fe_3O_4 nanoparticles. The nanoparticles tend to aggregate and form Fe_3O_4 nanocrystal clusters, driven by the minimization of interfacial energy [34] and the magnetic dipole–dipole interaction. Due to the obvious difference of polarity between EDA and EG, EDA can act as the surfactant in EG to form a layer on the surface of Fe_3O_4 nanocrystals and induce the assembly and growth of Fe_3O_4 nanocrystal clusters, similar to those surfactants used in the hydrothermal system to control the growth of nanostructures. As a result, cauliflower-like Fe_3O_4 hierarchical microstructures in EG solution might form under solvothermal conditions.

As one of the important crystal growth mechanisms, oriented assembly has been extensively investigated in aqueous solutions. Compared to the fast nucleation and aggregation growth in aqueous solution, the nanocrystals aggregated in the EG solution are kinetically slower due to fewer surface hydroxyls and greater viscosity, thus allowing the nanocrystals to rotate adequately to find the low-energy configuration interface and form perfectly oriented assemblies [35]. As a result, the cauliflower-like Fe_3O_4 hierarchitectures organized so well that they exhibited the feature of single crystals. Furthermore, when the surface-capped nanocrystals were used as building blocks, they were difficult to assemble into compact single-crystal structure so that the products with mesoporous-like structure were obtained [36].

The magnetic properties of the as-obtained Fe_3O_4 samples were investigated with a vibrating sample magnetometer (VSM) at room temperature in the applied magnetic field sweeping from −10 to 10 kOe. The hysteresis loops of the as-synthesized Fe_3O_4 samples are exhibited in Fig. 9. It can be seen from Fig. 9 that the saturation magnetizations (M_s) are 85, 68 and 65 emu/g for Fe_3O_4 solid microspheres, hollow microspheres, and cauliflower-like hierarchical microstructures, respectively. The saturation magnetization for Fe_3O_4 hollow microspheres and cauliflower-like hierarchical microstructures are also expected to be lower than for the corresponding bulk (M_s=92 emu/g) [37]. Compared to the coercivity value (H_c) of Fe_3O_4 solid microspheres (ca. 47 Oe) and hollow microspheres (ca. 94 Oe), the cauliflower-like Fe_3O_4 hierarchical

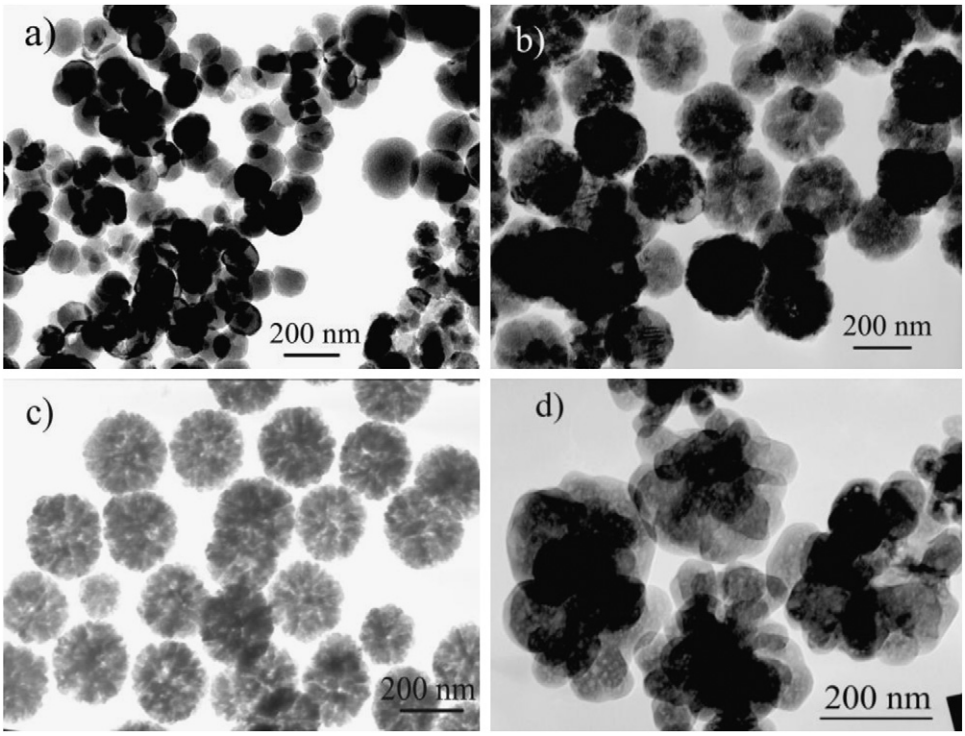

Fig. 7. TEM images of the products obtained at different reaction times: (a) 8.5 h, (b) 10 h, (c) 12 h, and (d) 16 h.

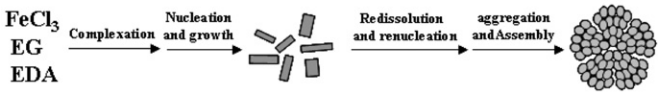

Fig. 8. Schematic illustration of the formation of cauliflower-like Fe_3O_4 hierarchical microstructures.

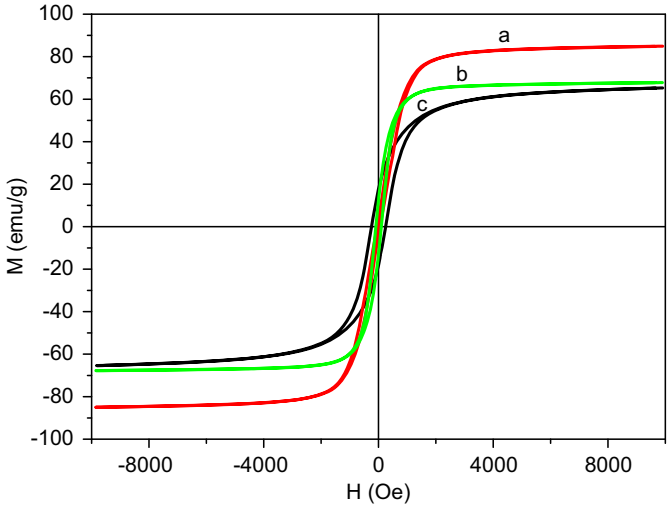

Fig. 9. Room temperature magnetization curves for the as-obtained samples: (a) the solid spheres, (b) the hollow spheres, and (c) cauliflower-like Fe_3O_4 hierarchical microstructures.

microstructures exhibit an enhanced value (ca. 247 Oe), which differ from that of the Fe_3O_4 nanooctahedra (ca. 74 Oe), nanoroses (ca. 225 Oe), dendritic microstructures (271.4 Oe), and so on. It is well known that the size, structure, and shape may affect the magnetic properties of the product. The different magnetizations and coercivities of as-synthesized products may be attributed to the different morphologies and structures of Fe_3O_4 particles.

4. Conclusion

In summary, cauliflower-like Fe_3O_4 hierarchical microstructures have been synthesized using a solvothermal growth method. This method is based on a mild and direct reaction between $FeCl_3 \cdot 6H_2O$ and EDA in EG solution. The results of XRD, SEM, and TEM show that the as-synthesized samples have cauliflower-like hierarchical microstructures with the average size of about 240 m in diameter. This cauliflower-like hierarchical microstructure comprises of nanocrystal clusters that are 20–50 nm in scale. According to the results, it is reasonable to assume that EDA plays an important role in determining the shape of the Fe_3O_4 architectures. Magnetic properties of cauliflower-like Fe_3O_4 hierarchical microstructures show a relatively low saturation magnetization of 65 emu/g and an enhanced coercive force of 247 Oe, which may be attributed to their morphology and structure. The as-prepared Fe_3O_4 hierarchical microstructures are expected to be useful in catalysis, magnetic, biological, and sensing related fields.

Acknowledgments

This work was supported by the Overseas Outstanding Scholar Foundation of Chinese Academy of Sciences (Grant nos.: 2005-1-3 and 2005-2-1), Shanghai Municipal Natural Science Foundation (Grant no.:10ZR1412200), the Specialized Research Fund for Outstanding Young Teachers in Shanghai Higher Education Institutions (Grant no.: egd08013), and the Innovation Program of the Shanghai Municipal Education Commission (Grant no.: 10YZ200). We also gratefully thank Prof. Shao-Yun Fu for helpful discussion.

References

[1] G.F. Goya, T.S. Berquo, F.C. Fonseca, J. Appl. Phys. 94 (2003) 3520.
[2] F. Caruso, M. Spasova, A. Susha, M. Giersig, R.A. Caruso, Chem. Mater. 13 (2001) 109.
[3] T. Hyeon, Chem. Commun. 8 (2003) 927.

[4] T. Hyeon, Y. Chung, J. Park, S.S. Lee, Y.W. Kim, B.H. Park, J. Phys. Chem. B 106 (2002) 6831.
[5] T. Hyeon, S.S. Lee, J. Park, Y. Chung, H.B. Na, J. Am. Chem. Soc. 123 (2001) 12798.
[6] S. Yu, M. Yoshimura, Adv. Funct. Mater. 12 (2002) 9.
[7] S. Lian, E. Wang, Z. Kang, Y. Bai, L. Gao, M. Jiang, C. Hu, L. Xu, Solid State Commun. 129 (2004) 485.
[8] J. Wan, X. Chen, Z. Wang, X. Yang, Y. Qian, J. Cryst. Growth 276 (2005) 571.
[9] J. Wang, Q. Chen, C. Zeng, B. Hou, Adv. Mater. 16 (2004) 137.
[10] Z. Huang, Y. Zhang, F. Tang, Chem. Commun. (2005) 342.
[11] Z. Liu, D. Zhang, S. Han, C. Li, B. Lei, W. Lu, J. Fang, C. Zhou, J. Am. Chem. Soc. 127 (2005) 6.
[12] F. Liu, P. Cao, H. Zhang, J. Tian, C. Xiao, C. Shen, J. Li, H. Gao, Adv. Mater. 17 (2005) 1893.
[13] C. Hu, Z. Gao, X. Yang, Chem. Phys. Lett. 429 (2006) 513.
[14] X.M. Liu, S.Y. Fu, H.M. Xiao, Mater. Lett. 60 (2006) 2779.
[15] W. Yu, T. Zhang, J. Zhang, X. Qiao, L. Yang, Y. Liu, Mater. Lett. 60 (2006) 2998.
[16] D. Yu, X. Sun, J.i Zou, Z. Wang, F. Wang, K. Tang, J. Phys. Chem. B 110 (2006) 21667.
[17] L.P. Zhu, H.M. Xiao, W.D. Zhang, G. Yang, S.Y. Fu., Cryst. Growth. Des. 8 (2008) 957.
[18] L.S. Zhong, J.S. Hu, H.P. Liang, A.M. Cao, W.G. Song, L.J. Wan, Adv. Mater. 18 (2006) 2426.
[19] J. Ge, Y. Hu, M. Biasini, W.P. Beyermann, Y. Yin, Angew. Chem. Int. Ed. 46 (2007) 4342.
[20] J. Ge, Y. Hu, Y. Yin, Angew. Chem. Int. Ed. 46 (2007) 7428.
[21] J. Liu, Z. Sun, Y. Deng, Y. Zou, C. Li, X. Guo, L. Xiong, Y. Gao, F. Li, D. Zhao, Angew. Chem. Int. Ed. 48 (2009) 5875.
[22] Z. Ai, K. Deng, Q. Wan, L. Zhang, S. Lee, J. Phys. Chem. C 114 (2010) 6237.
[23] G. Sun, B. Dong, M. Cao, B. Wei, C. Hu, Chem. Mater. 23 (2011) 1587.
[24] I.J. Bruce, J. Taylor, M. Todd, M.J. Davies, E. Borioni, C. Sangregorio, T. Sen, J. Magn. Magn. Mater. 284 (2004) 145.
[25] Z. Ma, Y. Guan, H. Liu, J. Polymer Sci: Part A: Polymer Chem. 43 (2005) 3433.
[26] Z. Zhong, Y. Yin, B. Gates, Y. Xia, Adv. Mater. 12 (2000) 206.
[27] S.W. Kim, M. Kim, W.Y. Lee, T. Hyeon, J. Am. Chem. Soc. 124 (2002) 7642.
[28] M. Wen, Y.F. Wang, F. Zhang, Q.S. Wu, J. Phys. Chem. C 113 (2009) 5960.
[29] L.H. Zhang, H.Q. Yang, J. Yu, F.H. Shao, L. Li, F.H. Zhang, H. Zhao, J. Phys. Chem. C 113 (2009) 5434.
[30] M.R. Kim, D.J. Jang, Chem. Commun. (2008) 5218.
[31] X.J. Wang, K. Han, F.Q. Wan, Y.J. Gao, K. Jiang, Mater. Lett. 62 (2008) 3509.
[32] H. Tang, J.G. Yu, X.F. Zhao, J. Alloys Compds. 460 (2008) 513.
[33] U. Pal, P. Santiago, J. Phys. Chem. B 109 (2005) 15317.
[34] C. Wu, Y. Xie, L. Lei, S. Hu, C. OuYang, Adv. Mater. 18 (2006) 1727.
[35] A.P. Alivisatos, Science 289 (2000) 736.
[36] T. He, A. Chen, X. Jiao, Chem. Mater. 16 (2004) 737.
[37] D.H. Han, J.P. Wang, H.L. Luo, J. Magn. Magn. Mater. 136 (1994) 176.